Article

Reversible Oxidative Addition and Reductive Elimination of Fluorinated Disulfides at Gold(I) Thiolate Complexes: A New Ligand Exchange Mechanism

Robert E. Bachman, Sheri A. Bodolosky-Bettis, Chelsea J. Pyle, and Margaret Anne Gray

J. Am. Chem. Soc., **2008**, 130 (43), 14303-14310 • DOI: 10.1021/ja805266r • Publication Date (Web): 01 October 2008

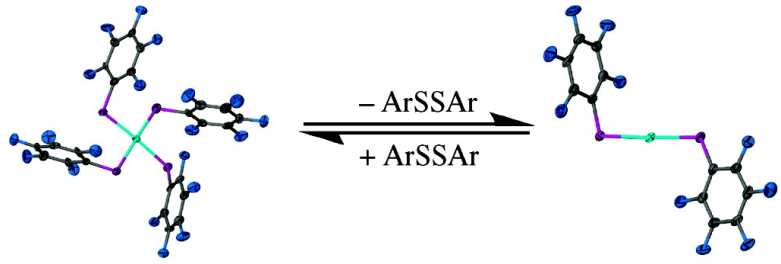

J|A|C|S
ARTICLES

Published on Web 10/01/2008

Reversible Oxidative Addition and Reductive Elimination of Fluorinated Disulfides at Gold(I) Thiolate Complexes: A New Ligand Exchange Mechanism

Robert E. Bachman,*,§ Sheri A. Bodolosky-Bettis,‡ Chelsea J. Pyle,§ and Margaret Anne Gray§

Departments of Chemistry, The University of the South, 735 University Avenue, Sewanee, Tennessee 37383, and Georgetown University, Box 571227, Washington, D.C. 20057-1227

Received July 8, 2008; E-mail: rbachman@sewanee.edu

Abstract: Reaction of $HAuCl_4 \cdot 3H_2O$ with excess HSAr (Ar = C_6F_5 or C_6F_4H) in ethanol, followed by addition of $[Et_4N]Cl$, produced $[Et_4N][Au(SAr)_4]$ (Ar = C_6F_5 (**1a**) or C_6F_4H (**1b**)) as red crystalline solids in high yield. These complexes are rare examples of homoleptic gold(III) thiolate complexes. The crystal structures **1** show square planar geometry at the gold center with elongated Au−S bonds. Both complexes undergo reversible reductive elimination/oxidative addition processes in solution via thermal and photochemical pathways. Equilibrium constant and photostationary state measurements indicate that the relative importance of the two pathways depends on the nature of the aromatic groups. The metal-containing reductive elimination products, $[Et_4N][Au(SAr)_2]$ (Ar = C_6F_5 (**2a**) or C_6F_4H (**2b**)), were confirmed by both independent synthesis and crystallographic characterization. Cross-reactions between either **1** or **2** and various disulfides led to ligand exchange via an addition−elimination process, a previously unknown reaction pathway for ligand exchange at gold(I) centers.

Introduction

As can be seen in the widely varied occurrences of gold thiolate species in the literature, sulfur-based ligands play a central role in the chemistry of gold, particularly in its reduced states of gold(I) and gold(0).[1] For example, thiols are commonly used to passivate and/or modify gold nanoparticles[2] and to form robust self-assembled monolayer assemblies on gold surfaces.[3] Thiols are also a key component in the formulation of gilding inks.[4] In essentially all of these applications, ligand substitution reactions are critical for selective patterning of surfaces or for tailoring other physical properties of the final system.[2−4] Despite the widespread use of such reactions, little is known about the mechanism of the substitution process.

Gold thiolates also play a central role in the biological chemistry of gold. Gold(I) thiolate species have been used as antiarthritic treatments for almost 80 years.[5] More recently, there have been reports suggesting that gold complexes containing gold(III) as well as gold(I) display antitumor and/or antimalarial behavior.[6] Interestingly, despite their long clinical use and intensive research by numerous groups, the precise mode of action of gold-based drugs *in vivo* remains elusive and likely involves diverse targets including transcription factors and cellular redox modulators.[7] One generally accepted paradigm is that many of the administered gold(I) thiolate complexes are rapidly undergoing ligand exchange processes with proteins, such as serum albumin, that possess available cysteine residues via a simple nucleophilic displacement mechanism (eq 1).

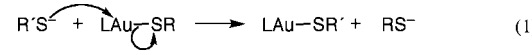

(1)

While there is substantial evidence to support this mechanism, there are some intriguing reports in the literature that hint that

§ The University of the South.
‡ Georgetown University.

(1) Shaw, C. F., III. The Biochemistry of Gold. In *Gold: Progress in Chemistry, Biochemistry, and Technology*; Schmidbaur, H., Ed.; Wiley: Chichester, 1999; pp 259−308.
(2) (a) Dolamic, I.; Gautier, C.; Boudon, J.; Shalkevich, N.; Burgi, T. *J. Phys. Chem. C* **2008**, *112*, 5816–5824. (b) Tao, A. R.; Habas, S.; Yang, P. D. *Small* **2008**, *4*, 310–325.
(3) (a) Heimel, G.; Romaner, L.; Bredas, J. L.; Zojer, E. *Langmuir* **2008**, *24*, 474–482. (b) Ulman, A. *Acc. Chem. Res.* **2001**, *34*, 855–863. (c) Schlenoff, J. B.; Li, M.; Ly, H. *J. Am. Chem. Soc.* **1995**, *117*, 12528–12536.
(4) Bishop, P. T. *Gold Bull.* **2002**, *35*, 89–98.
(5) (a) Forestier, J. *J. Lab. Clin. Med.* **1935**, *20*, 827–840. (b) Smith, W. E.; Reglinski, J. Gold Drugs Used in the Treatment of Rheumatoid Arthritis. In *Perspectives on Bioinorganic Chemistry Vol. 1*; Dilworth, J. R., Hay, R. W., Nolan, K. B., Eds.; JAI Press Ltd.: Stamford, CT, 1991; pp 183−208. (c) Fricker, S. P. *Gold Bull.* **1996**, *29*, 53–59. (d) Smith, W. E.; Reglinski, J. *Metal-Based Drugs* **1994**, *1*, 497–507. (e) Shaw, C. F. *Chem. Rev.* **1999**, *99*, 2589–2600.
(6) (a) Arizti, M. P.; Garcia-Orad, A.; Sommer, F.; Silvestro, L.; Massiot, P.; Chevallier, P.; Gutierrez-Zorrilla, J. M.; Colacio, E.; Martinez de Pancorbo, M.; Tapiero, H. *Anticancer Res.* **1991**, *11*, 625–628. (b) Navarro, M.; Pérez, H.; Sánchez-Delgado, R. A. *J. Med. Chem.* **1997**, *40*, 1937–1939. (c) Pillarsetty, N.; Katti, K. K.; Hoffman, T. J.; Volkert, W. A.; Katti, K. V.; Kamei, H.; Koide, T. *J. Med. Chem.* **2003**, *46*, 1130–1132. (d) Messori, L.; Abbate, F.; Marcon, G.; Orioli, P.; Fontani, M.; Mini, E.; Mazzei, T.; Carotti, S.; O'Connell, T.; Zanello, P. *J. Med. Chem.* **2000**, *43*, 3541–3548.
(7) (a) Urig, S.; Fritz-Wolf, K.; Reau, R.; Herold-Mende, C.; Toth, K.; Daoid-Charvet, E.; Becker, K. *Angew. Chem., Int. Ed.* **2006**, *45*, 1881–1886. (b) Gunatilleke, S. S.; Barrios, A. M. *J. Med. Chem.* **2006**, *49*, 3933–3937. (c) Larabee, J. L.; Hocker, J. R.; Hanas, J. S. *Chem. Res. Toxicol.* **2005**, *18*, 1943–1954. (d) Chircorian, A.; Barrios, A. M. *Bioorg. Med. Chem. Lett.* **2004**, *14*, 5113–5116. (e) Stoyanov, J. V.; Brown, N. L. *J. Biol. Chem.* **2003**, *278*, 1407–1410. (f) Handel, M. L.; Watts, C. K. W.; DeFazio, A.; Day, R. O.; Sutherland, R. L. *Proc. Natl. Acad. Sci. U.S.A.* **1995**, *92*, 4497–4501.

this might be an incomplete picture. For example, Sadler and co-workers reported finding the mixed Cys-STg (STg = thioglucose) disulfide species in preparations of Auranofin and bovine serum albumin.[8] Shaw and co-workers have also observed reactivity between cationic gold(I) complexes and disulfide-protected albumin.[9] They have also recently reported the formation of the disulfide GSSG as a byproduct of the glutathione reduction of $[Au(CN)_4]^-$ via the heteroleptic gold(III) complex $[Au(CN)_2(SG)_2]^-$ (eq 2).[10]

$$[Au(CN)_4]^- + G^-SH \xrightarrow[-2HCN]{} [Au(CN)_2(SG)_2]^{3-} \rightarrow [Au(CN)_2]^- + GSSG^{2-} \quad (2)$$

Additionally, multiple groups have also demonstrated the cleavage of disulfide linkages by gold(I) in the gas phase.[11] Finally, Ashraf and Isab have shown that both $(R_3P)_2Au^+$ and $[Au(I)STm]_n$ (STm = thiomalate) are capable of cleaving disulfides or diselenides in solution, with the mixed species RSeSTm observed in the latter case.[12]

Given this wide array of results, it is intriguing that Bruce and co-workers have demonstrated that gold thiolate complexes, including currently used gold drugs, are capable of mediating thiol−disulfide exchange reactions.[13] In their work, they have hypothesized that gold(III) species may form as reaction intermediates, which suggests that gold(III) species may play a significant role in the chemistry of gold thiolates generally. Numerous other groups have also found evidence for the formation of gold(III) species *in vivo*.[14] For example, De Wall et al. have reported that gold(III) is highly effective at altering the conformation of MHC proteins, which are known to play an important role in immune function.[15]

An inherent difficulty in studying the behavior of gold(III) thiolate species, as well as the possible role of gold(III) as an *intermediate* in the reactions of gold(I), is the facile and rapid reduction of gold(III) to gold(I) that is typically observed upon addition of thiols. However, in a pair of little-noticed papers,[16] Muller et al. and Peach reported preliminary evidence suggesting that highly electron-deficient thiols might be sufficiently less capable of reducing gold(III) to allow for the isolation of homoleptic gold(III) thiolate complexes. In this report, we build on their initial observations by isolating and structurally characterizing two examples of homoleptic gold(III) thiolate complexes with highly fluorinated ligands. To our knowledge, only one other homoleptic gold(III) thiolate complex has been isolated to date. This work also provides the first unambiguous example of the reductive elimination of disulfide from a gold(III) center and, perhaps more significantly, the reverse process of oxidative addition of a disulfide to a *single* gold(I) center. In light of these findings, we propose a novel addition−elimination mechanism for ligand substitution reactions at gold(I) centers, which is likely to have relevance to the reactivity of gold(I) complexes in a variety of settings, including biological ones.

Experimental Procedures

Materials. All experiments were carried out in air unless otherwise noted. Solvents were reagent grade or better and used as received from the vendor. $HAuCl_4 \cdot 3H_2O$ (Strem Chemicals), C_6F_5SH (Aldrich), 2,3,5,6-C_6F_4HSH (Aldrich; referred to hereafter as HSC_6F_4H-p), $Et_4NCl \cdot XH_2O$ (Aldrich), bentonite clay (Acros), and trifluoroacetic acid (Acros) were purchased from the noted suppliers and used as received. Me_2SAuCl was prepared by direct reaction of Me_2S and $HAuCl_4 \cdot 3H_2O$ in ethanol. The disulfides, RSSR (**3**), were prepared by the method described by Meshram.[17]

Physical Measurements. ^1H, ^{19}F, and ^{13}C NMR spectra were recorded in the solvent specified on a Varian Gemini spectrometer operating at 300 (^1H), 282 (^{19}F), and 75.45 MHz (^{13}C). The ^1H and ^{13}C chemical shifts were internally referenced to TMS ($\delta = 0$ ppm), while the ^{19}F chemical shifts were externally referenced to neat trifluoroacetic acid ($\delta = 0$ ppm). UV−visible spectra for routine characterization were recorded on a Hewlett-Packard 8453 diode array spectrophotometer in the solvents indicated. Irradiation experiments to determine the photostationary states were performed using an Osram XBO 450 W lamp connected to a PTI monochromator, model 101/102. Slit widths of entrance and exit were both set to 5 mm, corresponding to 20 nm of resolution. Sample temperature was maintained by use of a water filter. Following irradiation, UV−visible spectra were recorded on a Cary 300 Bio UV−vis dual-beam scanning spectrophotometer. Electrochemical measurements were performed using a CH Instruments model 630A potentiostat system with a glassy carbon working electrode, a platinum auxiliary electrode, and a nonaqeuous (CH_3CN) Ag/$AgNO_3$ reference electrode (590 mV vs NHE). The measurements were carried out at room temperature in acetonitrile solutions containing ca. 0.1 M $[(n\text{-}Bu)_4N][PF_6]$ as the supporting electrolyte. All processes were electrochemically irreversible, and as such, the values reported are the peak currents, adjusted so as to be relative to NHE, for the process in question.

Determination of Thermal Equilibrium Constants. "Normal" equilibrium constants—those determined under ambient lighting—were determined by preparing solutions with known concentrations of **1**, or **1** and the corresponding disulfide **3**, in acetone-d_6. The mixtures were monitored by ^{19}F NMR until the integrals of the signals achieved constant values. Alternatively, the concentration of **1** in solution could be monitored by UV−vis spectrometry at 470 nm until a constant value was observed. To determine "dark" equilibrium constants (i.e., in the absence of ambient light), solutions of known concentrations of **1** were prepared in acetone-d_6 in photographic dark room (red light) conditions. Aliquots (1 mL) of

(8) Orla, M. N. D.; Sadler, P. J.; Tucker, A. *J. Am. Chem. Soc.* **1992**, *114*, 1118–1120.
(9) (a) Isab, A. A.; Hormann, A. L.; Hill, D. T.; Griswold, D. E.; DiMartino, M. J.; Shaw, C. F., III *Inorg. Chem.* **1989**, *28*, 1321–1326. (b) Roberts, J. R.; Xiao, J.; Schliesman, B.; Parsons, D. J.; Shaw, C. F., III *Inorg. Chem.* **1996**, *35*, 424–433.
(10) Yangyuoru, P. M.; Webb, J. W.; Shaw, C. F., III *J. Inorg. Biochem.* **2008**, *102*, 584–593.
(11) (a) Lioe, H.; Duan, M.; O'Hair, R. A. J. *Rapid. Commun. Mass Spectrom.* **2007**, *16*, 2727–2733. (b) Gunawardena, H. P.; O'Hair, R. A. J.; McLuckey, S. A. *J. Proteome Res.* **2006**, *9*, 2087–2092.
(12) (a) Ahmad, S.; Isab, A. A.; Wazeer, M. I. M. *Inorg. React. Mech.* **2002**, *1*−*2*, 95–102. (b) Ashraf, W.; Isab, A. A. *J. Coord. Chem.* **2004**, *57*, 337–346.
(13) (a) Mohamed, A. A.; Chen, J.; Bruce, A. E.; Bruce, M. R. M. *Inorg. Chem.* **2003**, *42*, 2203–2205. (b) Mohamed, A. A.; Abdou, H. E.; Chen, J.; Bruce, A. E.; Bruce, M. R. M. *Comm. Inorg. Chem.* **2002**, *23*, 321–334. (c) Chen, J.; Jiang, T.; Wei, G.; Mohamed, A. A.; Homrighausen, C.; Bauer, J. A. K.; Bruce, A. E.; Bruce, M. R. M. *J. Am. Chem. Soc.* **1999**, *121*, 9225–9226. (d) DiLorenzo, M.; Ganesh, S.; Tadayon, L.; Chen, J.; Bruce, M. R. M.; Bruce, A. E. *Metal-Based Drugs* **1999**, *6*, 247–253.
(14) (a) Shaw, C. F., III; Schraa, S.; Gleichmann, E.; Grover, Y. P.; Dunemann, L; Jagarlamundi, A. *Metal-Based Drugs* **1994**, *1*, 351–362. (b) Takhashi, K.; Griem, P.; Goebel, C.; Gonzalez, J.; Gleichmann, E. *Metal-Based Drugs* **1994**, *1*, 483–496. (c) Verwilghen, J.; Kingsley, G. H.; Gambling, J.; Panayi, G. S. *Arthritis Rheum.* **1992**, *35*, 1413–1418.
(15) De Wall, S. L.; Painter, C.; Stone, J. D.; Bandaranayake, R.; Wiley, D. C.; Mitchison, T. J.; Stern, L. J.; DeDecker, B. S. *Nature Chem. Biol.* **2006**, *2*, 197–201.
(16) (a) Muller, M.; Clark, R. J. H.; Nyholm, R. S. *Transition Met. Chem.* **1978**, *3*, 369–377. (b) Peach, M. E. *Can. J. Chem.* **1968**, *46*, 2699.
(17) Meshram, H. M. *OPPI Briefs* **1993**, *25* (2), 232–233.

the solutions were transferred to amber-colored NMR tubes and wrapped in foil. The ^{19}F NMR spectrum of each sample was taken once daily, and the integrals of the signals were monitored until a constant value was established.

Determination of Photostationary States. Solutions of known concentrations of **1** were prepared in acetone under red light conditions. A small aliquot (~3 mL) of the solution was transferred to a 1 cm quartz cuvette and capped. The sample was placed 1 cm from the monochromator opening and irradiated for 2 h at room temperature with light of either 470 or 350 nm. After 2 h, the absorbance at 470 nm was monitored periodically (typically every 15 min) until it remained constant. The determination of this photostationary state was repeated three times for each sample at both 470 and 350 nm.

X-ray Crystallography. All X-ray data were collected on a Bruker-AXS SMART CCD diffractometer at −100 °C using methods previously described elsewhere.[18] The essential experimental details for all structures are provided in the Supporting Information. Final unit cell parameters were calculated by least-squares refinement of 4546 (**1a**), 6868 (**2a**), 5958 (**1b·EtOH**), and 1220 (**2b**) strong reflections taken from the entire data sets. The data were corrected for Lorentz and polarization effects, and an absorption correction was applied on the basis of equivalent reflection measurements using Blessing's method as incorporated into the program SADABS.[19] The structures were solved using direct methods and refined against F^2 by full-matrix least-squares methods using the programs incorporated into the SHELXTL/PC suite and XSEED.[20] All non-hydrogen atoms were refined anisotropically, while hydrogen atoms were added in calculated positions using a standard riding model. The solvent molecule located in the lattice of **1b·EtOH** is severely disordered around an inversion center. Given the difficulty in establishing reliable carbon and oxygen atom positions, no attempt was made to model the hydrogen atom positions of the solvent molecule. The less than ideal model of this solvent molecule does not affect the chemically significant structural information, as the bonding parameters for **1b** remain unchanged within error when the solvent positions are completely omitted from the model.

Preparation of [Et$_4$N][Au(SC$_6$F$_5$)$_4$] (1a). F_5C_6SH (0.45 mL, 3.4 mmol) was added dropwise to a solution of $HAuCl_4\cdot 3H_2O$ (290 mg, 0.74 mmol) in ethanol (15 mL). Immediately after completion of the thiol addition, 320 mg of $Et_4NCl\cdot XH_2O$ in water (5 mL) was added to the resulting red solution to produce a red microcrystalline precipitate that was isolated by filtration, washed with water, and dried in air. Yield: 579 mg (70%). ^{1}H NMR (acetone-d_6, ppm): 3.509 (q, 2H, J = 7.20 Hz), 1.391 (tt, 3H, J = 7.20, 1.80 Hz). ^{19}F{^{1}H} NMR (acetone-d_6, ppm): −51.925 (dd, 2F, J_{F-F} = 25.98, 7.63 Hz), −80.254 (t, 1F, J_{F-F} = 21.18 Hz), −87.129 (m, 2F). ^{13}C NMR (acetone-d_6, ppm): 148.3 (*o*-C, $^1J_{C-F}$ = 240 Hz), 146.7 (*m*-C, $^1J_{C-F}$ = 250 Hz), 119.3 (*i*-C, $^2J_{C-F}$ = 23 Hz), 140.7 (*p*-C, $^1J_{C-F}$ = 256 Hz), 52.5 (CH_2, $^1J_{C-H}$ = 144 Hz), 7.6 (CH_3, $^1J_{C-H}$ = 129 Hz). UV−vis (acetone): λ_{max} = 470 nm (ϵ ~3600 cm^{-1} M^{-1}), 353 nm (ϵ ~29 000 cm^{-1} M^{-1}). E_{red} = −302 mV vs NHE. Elemental analysis, calcd for $C_{32}H_{20}F_{20}S_4NAu$: C, 34.19; H, 1.78; N, 1.25. Found: C, 34.46; H, 1.76; N, 1.41. X-ray quality crystals were grown by slow evaporation of a methanolic solution of **1a** in air at room temperature.

Preparation of [Et$_4$N][Au(SC$_6$F$_4$H-p)$_4$] (1b). *p*-HF_4C_6SH (0.50 mL, 3.85 mmol) was added dropwise to a solution of $HAuCl_4\cdot 3H_2O$ (330 mg, 0.84 mmol) in ethanol (15 mL). $Et_4NCl\cdot XH_2O$ (350 mg) dissolved in water (5 mL) was immediately added to the resulting transparent red solution, resulting in a slight turbidity. The mixture was then placed in a freezer (−20 °C) for several days, during which time a red crystalline solid formed. The product was isolated by decanting off the remaining solvent and washing the solids with water and small aliquots of ether (3 × 2 mL). The solid was dried in air. Yield: 619 mg (70%). ^{1}H NMR (acetone-d_6, ppm): 7.789 (tt, 1H, $^3J_{H-F}$ = 10.2 Hz, $^4J_{H-F}$ = 7.7 Hz), 3.473 (t, 2H, J_{H-H} = 8.55 Hz), 1.843 (m, 2H), 1.448 (m, 2H), 0.989 (t, 3H, J_{H-H} = 7.20 Hz). ^{19}F{^{1}H} NMR (acetone-d_6, ppm): −52.79 (m, 2F), −63.76 (m, 2F). ^{13}C NMR (acetone-d_6, ppm): 147.8 (*o*-C, $^1J_{C-F}$ = 241 Hz), 146.7 (*m*-C, $^1J_{C-F}$ = 234 Hz), 125.2 (*i*-C, $^2J_{C-F}$ = 22 Hz), 100.0 (*p*-C, $^1J_{C-H}$ = 170 Hz, $^2J_{C-F}$ = 24 Hz), 52.5 (CH_2, $^1J_{C-H}$ = 144 Hz), 7.2 (CH_3, $^1J_{C-H}$ = 129 Hz). UV−vis (acetone): λ_{max} = 473 (ϵ ~4100 cm^{-1} M^{-1}), 355 nm (sh). E_{red} = −279 mV vs NHE. X-ray quality crystals were grown by slow evaporation of ethanolic solutions of **1b** in air at room temperature. This salt crystallizes as an ethanol solvate, which slowly loses solvent when removed from the mother liquor. Addition of Ph_4PBr rather than $Et_4NCl\cdot H_2O$ yields the corresponding $[Ph_4P]^+$ salt. Elemental analysis, calcd for $C_{48}H_{24}F_{16}S_4PAu$: C, 45.71; H, 1.91. Found: C, 45.48; H, 1.91.

Preparation of [Et$_4$N][Au(SC$_6$F$_5$)$_2$] (2a). Method 1. F_5C_6SH (0.068 mL, 0.510 mmol) was added to a solution of KOH (0.029 g, 0.510 mmol) in methanol (1 mL). This solution was then added to a suspension of Me_2SAuCl (0.075 g, 0.255 mM) in H_2O (~5 mL). Additional methanol (~10 mL) was added to dissolve any remaining solids. The solution was filtered, and $Et_4NCl\cdot H_2O$ (0.042 g, 0.255 mmol) was added to the filtrate to precipitate a white crystalline solid. The solid was washed with water (~10 mL) and ether (~1 mL). Yield: 0.0847 g (46%). ^{1}H NMR (acetone-d_6, ppm): 3.50 (q, 2H, J_{H-C} = 6.90 Hz), 1.40 (tt, 3H, J_{H-C} = 6.90, 1.80 Hz). ^{19}F{^{1}H} NMR (acetone-d_6, ppm): −55.62 (dd, 2F, J_{F-F} = 26.97, 5.79 Hz), −88.54 (m, 3H). ^{13}C NMR (acetone-d_6, ppm): 147.8 (*o*-C, $^1J_{C-F}$ = 240 Hz), 137.9 (*m*-C, $^1J_{C-F}$ = 232 Hz,), 119.0 (*i*-C, $^2J_{C-F}$ = 23 Hz), 138.4 (*p*-C, $^1J_{C-F}$ = 247 Hz), 53.0 (CH_2, $^1J_{C-H}$ = 144 Hz), 7.7 (CH_3, $^1J_{C-H}$ = 129 Hz). UV−vis (acetone): λ_{max} = 282 nm (ϵ ~17 000 cm^{-1} M^{-1}). E_{ox} = 1.35V vs NHE. Elemental analysis, calcd for $C_{20}H_{20}F_{10}S_2NAu$: C, 33.11; H, 2.78; N, 1.93. Found: C, 33.25; H, 2.85; N, 1.81.

Method 2. A solution of **1a** in acetone was allowed to stand until it changed from red to essentially colorless, typically at least 1 day. After the solution had turned colorless, ether was layered on top, and the solution was placed in a freezer (−20 °C) for approximately 1 week, after which time a small amount of colorless X-ray quality needle-shaped crystals of **2a** formed. All spectral features of these crystals are identical to those reported in method 1 above. Attempts to isolate and separate the gold complexes and disulfide remaining in solution led to intractable mixtures of the gold(III) salt and the disulfide.

Preparation of [Et$_4$N][Au(SC$_6$F$_4$H)$_2$] (2b). Method 1. Me_2SAuCl (0.077 g, 0.262 mmol) was suspended in methanol (10 mL), and a solution of *p*-HF_4C_6SH (0.062 mL, 0.523 mmol) in basic methanol (0.029 g, 0.523 mmol of KOH, in 5 mL of methanol) was added dropwise over a period of 2−3 min. After being stirred for 1 h, the colorless, transparent solution was filtered using a Whatman microfiber glass filter to remove small amounts of metallic gold and/or other insoluble impurities. $Et_4NCl\cdot XH_2O$ (0.087 g. 0.523 mmol) was added to the filtrate, and the solvent was removed in vacuo to yield a cream-colored solid. The solids were washed with water and then dried in air. Yield: 0.129 g (71%). ^{1}H NMR (acetone-d_6, ppm): 7.77 (tt, 1H, $^3J_{H-F}$ = 10.2 Hz, $^4J_{H-F}$ = 7.7 Hz), 3.51 (q, 2H, J_{H-H} = 7.50 Hz), 1.37 (tt, 3H, J_{H-H} = 7.50, 1.80 Hz). ^{19}F{^{1}H} NMR (acetone-d_6, ppm): −57.35 (m, 2F), −66.41 (m, 2F). ^{13}C NMR (acetone-d_6, ppm): 147.6 (*o*-C, $^1J_{C-F}$ = 235 Hz), 146.7 (*m*-C, $^1J_{C-F}$ = 244 Hz), 125.7 (*i*-C, $^2J_{C-F}$ = 23 Hz), 100.1 (*p*-C, $^1J_{C-H}$ = 170 Hz, $^2J_{C-F}$ = 24 Hz), 53.0 (CH_2, $^1J_{C-H}$ = 144 Hz), 7.7 (CH_3, $^1J_{C-H}$ = 129 Hz). UV−vis (acetone): λ_{max} = 298 nm (ϵ ~ 29 000 cm^{-1} M^{-1}). E_{ox} = 1.59 V vs NHE. Elemental analysis, calcd for $C_{20}H_{20}F_{10}S_2NAu$: C, 34.84; H, 3.22; N, 2.03. Found: C, 35.10; H, 3.05; N, 2.32.

Method 2. A solution of **1b** in ethanol was allowed to stand until it changed from red to pale orange or colorless, typically at least 1 day. Once the system had equilibrated, ether was layered on top, producing a small amount of X-ray quality crystals of **2b**

(18) Bachman, R. E.; Andretta, D. F. *Inorg. Chem.* **1998**, *37*, 5657–5663.
(19) Blessing, R. H. *Acta Crystallogr.* **1995**, *A51*, 33–38.
(20) (a) *SHELXTL-PC*, Version 5.10; Bruker AXS: Madison, WI, 1998. (b) Barbour, L. *XSEED*, 1999; http://www.x-seed.net/index.html.

Table 1. Average Equilibrium and Photostationary State Constants for **1**[a]

1a ⇆ 2a + 3a	
thermal equilibrium, dark	0.12[b]
thermal equilibrium, room light	0.13 (0.02)
photostationary state, 350 nm	0.16 (0.01)
photostationary state, 470 nm	0.19 (0.03)
1b ⇆ 2b + 3b	
thermal equilibrium, dark	ND
thermal equilibrium, room light	1.09 (0.12)
photostationary state, 350 nm	0.62 (0.10)
photostationary state, 470 nm	1.30 (0.10)

[a] The standard deviation is provided in parentheses. [b] Experiment only performed once due to extremely slow reaction kinetics.

Table 2. Reaction of **2** and $[PhSAuSPh]^-$ with Various Disulfides

$[ArS\text{-}Au\text{-}SAr]^-$		RSSR		products
2a	+	**3a**	→	**1a**
		3b		$[Au(SC_6F_5)_2(SC_6F_4H)_2]^-$
		PhSSPh		**2a** + RSSR
		p-$FC_6H_4SSC_6H_4F$		**2a** + RSSR
		p-$MeC_6H_4SSC_6H_4Me$		**2a** + RSSR
		$(AcMeCys)_2$		$[Au(AcMeCys)]_n$ + **3a**
2b	+	**3a**	→	$[Au(SC_6F_5)_2(SC_6F_4H)_2]^-$
		3b		**1b**
		PhSSPh		**2b** + RSSR
		p-$FC_6H_4SSC_6H_4F$		**2b** + RSSR
		p-$MeC_6H_4SSC_6H_4Me$		**2b** + RSSR
		$(AcMeCys)_2$		$[Au(AcMeCys)]_n$ + **3b**
$[PhSAuSPh]^-$	+	**3a**	→	**2a** + PhSSPh
		3b		**2b** + PhSSPh

as colorless needles. All spectral features of these crystals are identical to those reported in method 1 above. Attempts to isolate and separate the gold complexes and disulfide remaining in solution led to intractable mixtures of the gold(III) salt and the disulfide.

Reaction of 2a or 2b with ArSSAr: Typical Procedure. A small amount (0.03−0.04 mmol) of **2a** or **2b** was dissolved in approximately 5 mL of methanol. A solution of an equimolar amount of the disulfide dissolved in methanol (5 mL) was added in one portion, and the mixture was allowed to stand for a minimum of 30 min. The solvent was removed *in vacuo*, and the residue was taken up in acetone-d_6 and immediately characterized by NMR spectroscopy. The results of these reactions are summarized in Table 2.

Reaction of 2a with *N*-Acetyl-L-cystine Methyl Ester ($(AcMeCys)_2$). A small sample of **2a** or **2b** (15−25 mg) was dissolved in approximately 5 mL of methanol. A solution containing an excess (25−55 mg) of $(AcMeCys)_2$ (AcMeCys = *N*-acetyl-L-cysteine methyl ester) in 5 mL of methanol was added in one portion. The reaction was mixed and left to stand for 10 min, during which time a white, highly luminescent precipitate of $[Au(AcMeCys)]_n$ formed. The solid was isolated by filtration, washed with methanol and ether, and dried in air. The filtrate was concentrated *in vacuo* to yield a residue of $C_6F_5SSC_6F_5$ or $C_6F_4HSSC_6F_4H$, which was characterized by ^{19}F NMR. ^{19}F NMR (acetone-d_6, ppm) for reaction with **2a**: −54.61 (dd, 2F), −71.21 (t, 1F), −82.91 (m, 2F). Elemental analysis, calcd for $C_6H_{10}AuNO_3S$: C, 19.39; H, 2.70. Found: C, 19.44; H, 2.76.

Results

Synthesis. Unlike the results observed with most thiols, the reaction of $[AuCl_4]^-$ with either F_5C_6SH or p-HF_4C_6SH does not lead immediately to the formation of oligomeric gold(I) thiolate complexes typically seen in reactions of gold(III) salts with thiols. Rather, the initial result is the formation of a bright red solution from which $[Et_4N][Au(SAr)_4]$ (**1**: **a**, Ar = F_5C_6; **b**, Ar = p-HF_4C_6) (Scheme 1) can be isolated in high yield (typically 70% or better) via the addition of $[Et_4N]Cl$. Addition of other organic cations, such as Ph_4P^+, results in the formation of the corresponding salts. These complexes are soluble in most moderately polar organic solvents and insoluble in water and nonpolar organic solvents. As expected, given the large amount of HCl byproduct generated in the reaction, the final solution medium is quite acidic (pH ≤ 1 by indicator paper). Interestingly, **1a** and **1b** appear to be unreactive toward this high concentration of acid, most likely due to the low basicity of the electron-deficient thiolates. We have measured the pK_a's of F_5C_6SH and p-HF_4C_6SH as 4.18 and 4.21, respectively; moreover, it is reasonable to assume that these values are even lower when the thiol is bound to a metal ion.[21] For comparison, the pK_a of thiolphenol is 6.6, while that of aliphatic thiols is approximately 8.0.[22]

Scheme 1. Synthetic Routes for Preparing **1** and **2**

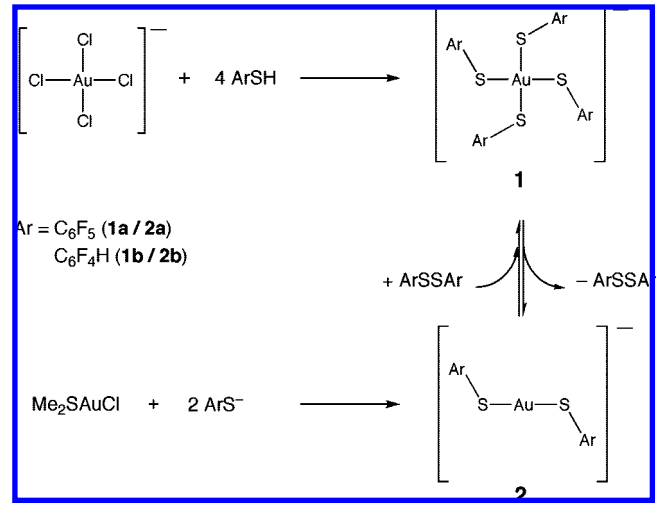

While stable in the solid-state, **1a** and **1b** undergo a reductive elimination to form their respective gold (I) complexes, $[Au(SAr)_2]^-$ (**2**), along with the corresponding disulfide, ArSSAr (**3**). Since complexes **1** are red and complexes **2** are colorless, the extent of this reaction can be qualitatively monitored by simple visible inspection; quantitative measurements can be made by UV−vis spectroscopy. Interestingly, even when a solution appears colorless, all three species (**1**, **2**, and **3**) can still be clearly identified in ^{19}F NMR spectra. Furthermore, evaporation of the solvent from such colorless mixtures results in the quantitative re-formation of **1**, by oxidative addition of **3** across the gold atom of **2**, yielding a red solid (Scheme 1).

While **2** may not be isolated from the reductive elimination reaction by solvent removal, these complexes can be isolated by addition of a nonpolar solvent, such as ether, to the mixture resulting from the reductive elimination process. Alternatively, samples of **2** can be prepared directly via the reaction of a suitable gold(I) precursor, such as Me_2SAuCl, with a stoichiometric quantity of the desired thiolate anion (see Scheme 1).

(21) (a) Bodolosky-Bettis, S. Gold Thiolates: Luminescent Properties and Reductive-Elimination/Oxidative Addition Processes. Ph.D. Thesis, Georgetown University, 2003. (b) Tachtman, M.; Markam, G. D.; Glusker, J. P.; George, P.; Bock, C. W. *Inorg. Chem.* **2001**, *40*, 4230–4241.

(22) (a) Jencks, W. P.; Salvesen, K. J. *Am. Chem. Soc.* **1971**, *93*, 4433–4436. (b) Mathews, C. K.; van Holde, K. E.; Ahern, K. G. *Biochemistry*, 3rd ed.; Addison Wesley: San Fransciso, 2000; p 128.

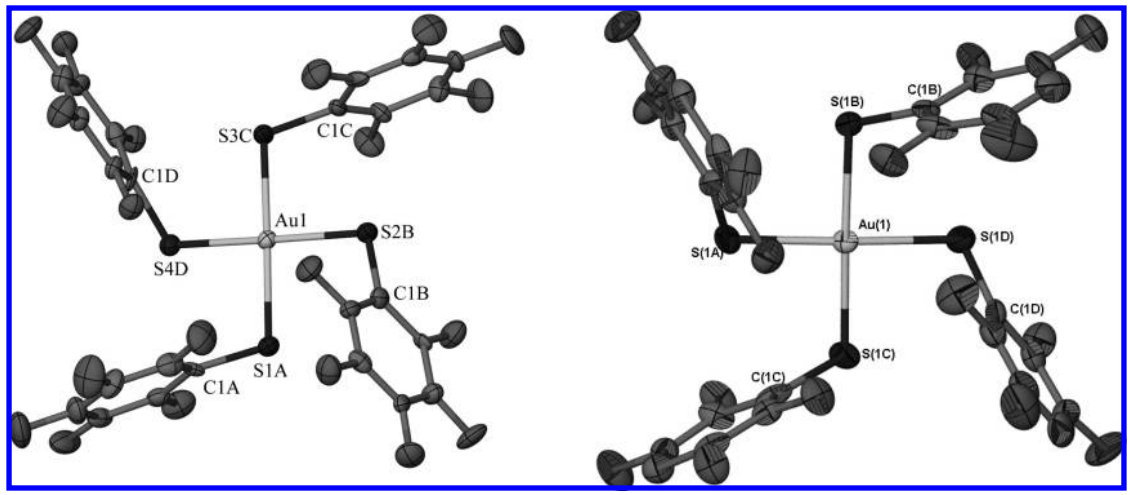

Figure 1. Structures of the anion portions of **1a** (left) and **1b** (right), including atom labeling scheme in the vicinity of the metal atom.

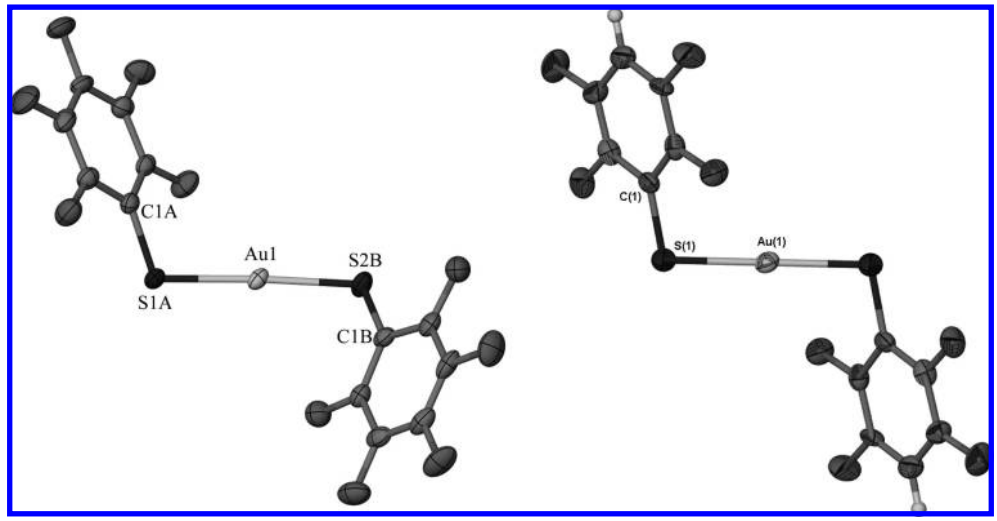

Figure 2. Structures of the anionic portions of **2a** (left) and **2b** (right), with the atom labeling scheme near the metal atom.

Reaction of **2** prepared in this manner with the appropriate disulfide (**3**) regenerates the characteristic red color of the gold(III) species, **1**.

Structure. Slow evaporation of methanolic or ethanolic solutions of **1** provided X-ray quality crystals of the red four-coordinate gold(III) complexes (Figure 1). In the case of **1b**, the salt crystallizes as an ethanol solvate. As expected for Au(III) complexes, the gold atoms in **1** are situated in a square planar coordination environment. The Au−S bond lengths in **1a** and **1b** are essentially identical (averages **1a**, 2.352 Å; **1b**, 2.349 Å). In both cases, they are also similar to those seen in the only other reported Au(III) complex with four monodentate thiolate ligands, $[Ph_4P][Au(Smetetraz)_4]\cdot 0.5H_2O$ (Smetetraz = 1-methyl-1,2,3,4-tetrazole-5-thiolate) (average 2.354 Å).[23] Interestingly, these distances are slightly longer than those observed in the mixed ligand complex $[Au_2Cl_4(\mu\text{-}SPh)_2]$ (average 2.334 Å), even though in this latter case the thiolates are bridging ligands.[24] One explanation for this difference is that the electron-deficient nature of the thiolate ligands in **1** results in slightly longer, and presumably weaker, metal−sulfur interactions. Alternatively, it is possible that the longer bonds are caused by the larger steric bulk of four fluorinated aromatic rings. The bond distances and angles within the ligands, including the aromatic C−C distances, are all within the expected ranges and show no significant or systematic variations between gold(I) and gold(III) or between degrees of fluoridation on the ring (see Supporting Information for detailed bond distances and angles).

X-ray quality crystals of **2** were prepared by dissolving **1** in acetone, allowing the reductive elimination process to proceed, and then isolated by layering the reaction mixture with ether and cooling to −20 °C. Crystallographic analysis of the resulting colorless needles confirmed the structures of **2** (Figure 2). As expected for two-coordinate gold(I) complexes, the geometry of the gold atoms in **2** is essentially linear (S−Au−S = 177.2° and 180°).[25] The Au−S distances (average **2a**, 2.2861 Å; **2b**, 2.2852 Å) are slightly longer than those observed in the corresponding perhydro complex, $[Ph_4P][Au(SPh)_2]$ (average 2.266 Å), but within the range observed (2.276−2.292 Å) for gold(I) thiolate complexes

(23) Lang, E. S.; Dahmer, M.; Abram, U. *Acta Crystallogr.* **1999**, *C55*, 854–856.
(24) Wang, S.; Fackler, J. P., Jr. *Inorg. Chem.* **1990**, *29*, 4404–4407.
(25) (a) Bartczak, T. J. *Acta Crystallogr.* **1985**, *C41*, 865–869. (b) Nomiya, K.; Noguchi, R.; Sakurai, T. *Chem. Lett.* **2000**, 274–275. (c) Watase, S.; Nakamoto, M.; Kitamura, T.; Kanehisa, N.; Kai, Y.; Yanagida, S. *J. Chem. Soc., Dalton Trans.* **2000**, 3585–3590.

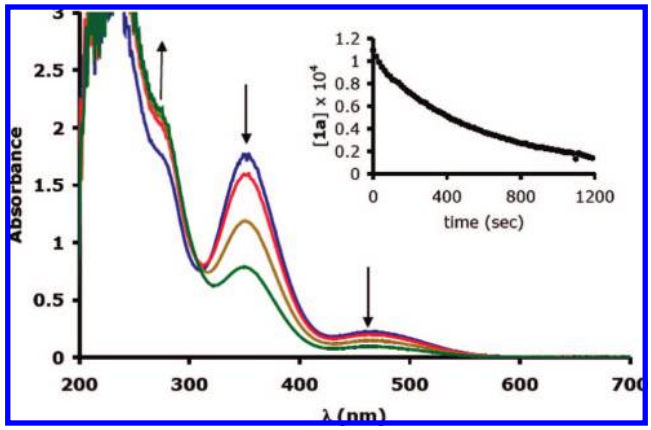

Figure 3. UV−vis spectra of **1a** over the course of 30 min, showing the disappearance of the peaks at 350 and 470 nm, as well as growth of a shoulder at 275 nm, as the reductive elimination occurs. Inset: plot of [**1a**] vs time at $\lambda = 468$ nm.

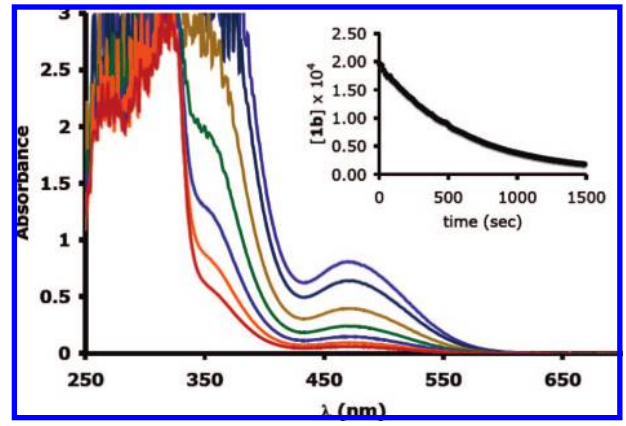

Figure 4. UV−vis spectra of **1b** over the course of 30 min showing the disappearance of the peaks at 350 and 470 nm as the reductive elimination occurs. Inset: plot of [**1b**] vs time at $\lambda = 468$ nm.

generally.[26] The slightly longer bonds observed for **2**, in relation to its perhydro derivative, are consistent with the idea put forth above regarding the impact of electron deficiency on metal−ligand bonding. Interestingly, the Au−S distances seen in **2** are significantly (0.065 Å) shorter than those in **1**, while the C−S and C−C bond lengths are essentially identical. The difference in the observed Au−S lengths for these two complexes is counter to expectations based on the relative sizes of the Au(III) and Au(I) centers. The most likely explanation for this result is the greater steric crowding of the ligands in the four-coordinate Au(III) complexes. This overall picture is also consistent with the lower stability of Au(III) thiolates.

Reductive Elimination. The solution state UV−visible spectra (Figure 3) of **1a** display two strong bands in the visible or near-UV region (468 nm, $\epsilon \sim 3600$ cm^{-1} M^{-1}; 350 nm, $\epsilon \sim 29\,000$ cm^{-1} M^{-1}). We have tentatively assigned the former transition to a metal-to-ligand charge transfer state, while the latter is likely a ligand-based transition. The only other features in the spectra are extremely intense ligand-centered transitions below 300 nm, which are common to all three species—**1**, **2**, and **3**—and hence of little diagnostic value. The spectrum of **1b** is similar (Figure 4) but with the higher 350 nm band overlapped with the ligand-centered bands and now appearing as a shoulder on the ligand-centered bands. This overlap is due to a red shift of the ligand-centered bands of both **2b** and **3b** associated with the loss of a fluorine atom (see Supporting Information). As **1** reductively eliminates **3** to form **2** (Scheme 2), both of the bands at 470 and 350 nm are seen to decrease in intensity. The presence of an isosbestic point at 310 nm in the spectra of **1a** supports the one-step nature of the reaction. As might be expected, kinetic data under these conditions are consistent with a first-order reaction for the reductive elimination process (Figures 3 and 4) with an apparent rate constant of 1.61×10^{-3} s^{-1} for **1a** and 1.58×10^{-3} for **1b**.

Scheme 2. Thermal and Photochemical Pathways for Reductive Elimination/Oxidative Addition Reactions

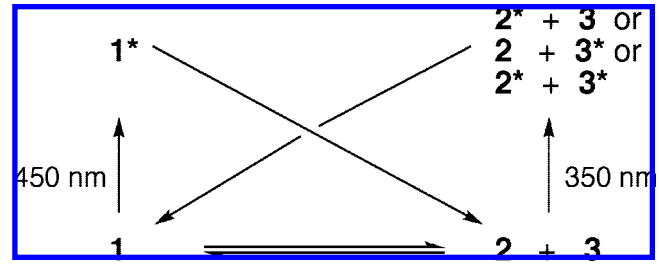

In contrast to the earlier reports by Muller et al.,[16a] the reductive elimination process appears to be independent of the presence of oxygen, as solutions of **1** rapidly convert to **2** in a rigorously oxygen-free environment (glovebox with <10 ppm O_2). However, the rate at which samples of **1** reach equilibrium was found to depend strongly on the presence of light. Under illumination by standard fluorescent lights, solutions of **1a** reach equilibrium in a few hours. In contrast, samples of **1a** kept in the dark require more than 10 days to achieve equilibrium. The impact of light is even more pronounced for **1b**. Samples exposed to room illumination reach equilibrium within a few hours, while those kept in the dark show almost no change, either visibly or by ^{19}F NMR spectroscopy, over the course of several weeks. These results suggest that the reductive elimination process involving **1** occurs via both a thermal and a photochemical pathway and, moreover, that the relative importance of these two pathways depends on the identity of the thiolate ligands.

In order to begin to probe the impact of illumination on the equilibria, we examined the equilibrium constant in the presence and in the absence of room light. For **1a** the value was essentially identical in both cases—$K_{light} = 0.13$ and $K_{dark} = 0.12$. While it was not possible to measure the equilibrium constant for **1b** under dark conditions, K_{light} was found to be 1.09. These results are consistent with electrochemical measurements. It is slightly more difficult to reduce **1a** than **1b** (−302 and −279 mV vs NHE, respectively) and, conversely, slightly easier to oxidize **2a** than **2b** (1.35 and 1.59 V vs NHE). Both the equilibrium measurements and the electrochemical results are consistent with the idea that greater electron deficiency at the thiolate ligand enhances the thermodynamic stability of the Au(III) complex. Indeed, we have been unable to isolate gold(III) thiolate complexes for any thiol with fewer than four

(26) For example, see: (a) Hunks, W. J.; Jennings, M. C.; Puddephatt, R. J. *Inorg. Chem.* **2000**, *39*, 2699–2702. (b) Tzeng, B.-C.; Schier, A.; Schmidbaur, H. *Inorg. Chem.* **1999**, *38*, 3978–3984. (c) Bishop, P.; Marsh, P.; Brisdon, A. K.; Brisdon, B. J.; Mahon, M. F. *J. Chem. Soc., Dalton Trans.* **1998**, 675–682. (d) Tzeng, B.-C.; Chan, C.-K.; Cheung, K.-K.; Che, C.-M.; Peng, S.-M. *Chem. Commun.* **1997**, 135–136. (e) Schneider, W.; Bauer, A.; Schmidbaur, H. *Organometallics* **1996**, *15*, 5445–5446. (f) Forward, J. M.; Bohmann, D.; Fackler, J. P., Jr.; Staples, R. J. *Inorg. Chem.* **1995**, *34*, 6330–6336.

Scheme 3. Equilibrium System of Oxidative Addition and Reductive Elimination Reactions Involving Gold(I) Dithiolate Complexes and Disulfides

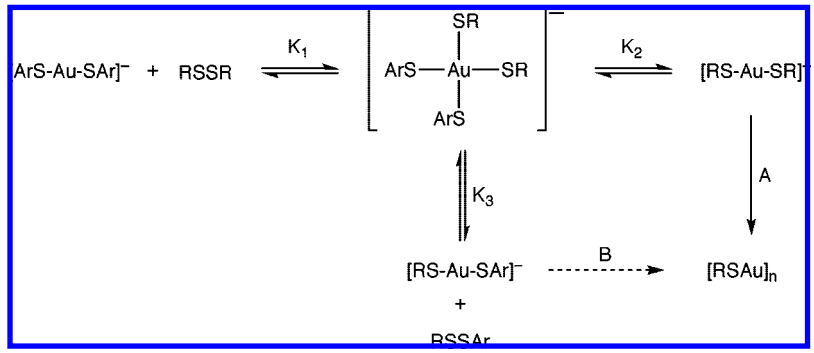

fluorine atoms, as such systems rapidly convert to either a bisdithiolate complex analogous to **2** or an insoluble oligomeric material with a generic formula of $[AuSR]_n$.[21a] Even though **1a** is thermodynamically more stable than **1b**, its more rapid equilibration with its reduced form (**2a**), particularly in the absence of light, implies a lower thermal activation energy for the more fluorinated complex (**1a**).

To further probe the role of light in these reactions, we also examined the photostationary state (PS) constants for **1a/b** at two wavelengths: 470 and 350 nm. The results of these experiments are summarized in Table 1. In the case of **1a**, the PS constant obtained at both wavelengths is identical within experimental error to both K_{light} and K_{dark}. For **1b**, irradiation at 350 nm results in a PS constant that is roughly half that seen for irradiation at 470 nm, while K_{light} is intermediate between the two values. The overall picture that can be developed from these results (Scheme 3) is that both the reductive elimination reaction of **1** and the reverse process involving oxidative addition of **3** across the gold center in **2** occur via both photochemical and thermal pathways. Furthermore, the more significant wavelength dependence of **1b** suggests that the photochemical pathway is more important in this case. This conclusion is consistent with the exceedingly slow rate of reaction observed for **1b** in the absence of light. While the precise structural/electronic reasons for the different behavior of **1a** and **1b** are not entirely clear, it has been suggested that the relative energy of π^*-based and σ^*-based excited states of fluorinated aromatic rings depends on the number of fluorine atoms attached to the ring.[27] Increasing numbers of fluorine atoms stabilize the σ^* states such that they become the more stable excited state when at least five fluorine atoms are present. Hence, it seems reasonable to conjecture that similar differences in excited states lead to the reactivity patterns seen in this system.

Oxidative Addition and Ligand Exchange. The outcomes of mixing **2** or the closely related species $[(PhS)_2Au]^-$ with a variety of disulfide species are summarized in Table 2. As expected, mixing **2a** with **3a** resulted in the re-formation of **1a**, while mixing **2b** with **3b** regenerated **1b**. The cross reactions of **2a** with **3b** or **2b** with **3a** resulted in a scrambling of the ligands at gold. These results were confirmed by ^{19}F NMR spectroscopy, which shows signals for both the symmetric (**3**) and asymmetric ($F_5C_6SSC_6F_4H$) disulfides, as well as a crystal structure of an Au(III) complex in which the para positions of the aromatic rings are a superposition of fluorine and hydrogen atoms in an approximately 2:1 ratio.[21a] The greater than 1:1 ratio (which would be expected for simple oxidative addition process) observed in this case clearly illustrates the dynamic nature of the addition−elimination process as well as the preferential stabilization of the gold(III) species by the more electron-deficient ligand.

Attempts to add more electron-rich disulfides across the Au(I) center of **2a** yielded no *apparent* reaction with one significant exception, *N*-acetyl-L-cystine methyl ester ($(AcMeCys)_2$). In this case the result was the rapid formation of an insoluble white solid consistent with the formula $[Au(AcMeCys)]_n$ by elemental analysis. This solid also displayed an intense red luminescence, consistent with similar oligomeric gold(I) species previously prepared in our laboratories.[28] In keeping with the preference for gold to selectively bind the more electron-deficient ligands, reactions of $[Au(SPh)_2]^-$ with **3a** or **3b** resulted in rapid and complete ligand exchange to yield **2a** or **2b**, respectively. Reactions of $[Au(SPh)_2]^-$ with other disulfides, such as $(p\text{-}FH_4C_6S)_2$ or $(p\text{-}CH_3H_4C_6S)_2$, have yielded complex mixtures, including oligomeric materials with a nominal formula of $[AuSAr]_n$, that have eluded complete identification to date.[21a]

Discussion

The surprising stability of the gold(III) tetrathiolate complexes (**1**) reported here is certainly due to the electron deficiency of the highly fluorinated thiolates employed. While such stability has been suggested before,[16] the formation of these complexes by oxidative addition of a disulfide to a gold(I) fragment has, to our knowledge, no precedent in the literature. Previously reported examples of oxidative addition at gold(I) typically involve addition of halogens or alkyl halides. Moreover, many of these examples involve the distinctly different process of addition across a pair of gold(I) centers to produce gold(II) (eq 3),[29] rather than addition across a single metal atom to yield a gold(III) center, as is seen in this work.

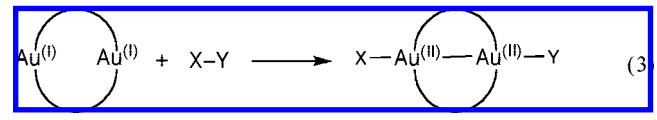

(27) Zgierski, M.; Fujiwara, T.; Lim, E. C. *J. Chem. Phys.* **2005**, *122*, 144312–144316.

(28) Bachman, R. E.; Bodolosky-Bettis, S. A.; Glennon, S. C.; Sirchio, S. A. *J. Am. Chem. Soc.* **2000**, *122*, 7146–7147.

(29) For recent examples, see: (a) Schuster, O.; Schmidbaur, H. *Inorg. Chim. Acta* **2006**, *359*, 3769–3775. (b) Schneider, D.; Schuster, O.; Schmidbaur, H. *Dalton Trans.* **2005**, 1940–1947. (c) Abdou, H. E.; Mohamed, A. A.; Fackler, J. P., Jr. *Inorg. Chem.* **2005**, *44*, 166–168. (d) Abdou, H. E.; Mohamed, A. A.; Fackler, J. P., Jr. *Z. Naturforsch. B: Chem. Sci.* **2004**, *59*, 1480–1482.

Comparing the reactivity of **1a** and **1b**, the loss of a fluorine atom in **1b** results in a significant increase in electron density at the ipso carbon of the aromatic ring. The latter can be easily observed by the significant shifts seen for the appropriate ^{13}C NMR signals: 20 ppm for **1a** and **1b**; 6 ppm for **2a** and **2b**. It is reasonable to assume that the increased electron density at the ipso carbon translates directly to an increase in electron density at the attached sulfur atom and, by extension, at the gold center. Such an increase in electron density should destabilize the higher gold oxidation state and lead to more facile reduction. This picture is consistent with the rapid reduction to gold(I) typically seen upon addition of thiols to gold(III) salts as well as our inability to isolate gold(III) complexes of di- or trifluorobenzenethiolates. In such cases, we observe rapid reduction to gold(I) and isolation of either a complex analogous to **2** or an insoluble oligomeric complex with a 1:1 metal-to-ligand ratio; the precise outcome depends on both the identity of the thiol and the reaction conditions.[21a] These results illustrate the sensitivity of the gold center to relatively small changes in the electronics of the ligand periphery.

While the complete mechanistic details of the addition and elimination processes have yet to be elucidated, the rapidity and reversibility of these processes under normal room illumination suggest an alternative mechanism for ligand substitution reactions at gold(I) centers generally, one that explains the seemingly anomalous behavior seen for NAMeCys. Conceptually, the addition of any disulfide to a solution of a gold(I) thiolate complex can generate an equilibrium between the gold(I) complex and the corresponding gold(III) species. The equilibrium constant for this process is set largely by the electron deficiency of the organic fragments of the disulfide and the ligands on the gold center. Greater electron deficiency on either group yields a larger equilibrium constant for the oxidative addition (or a smaller equilibrium constant for the reductive elimination). Moreover, as shown by the reactions of $[Au(SPh)_2]^-$ with **3**, the reductive elimination process favors elimination of the most electron-rich thiolates, an interpretation completely consistent with the results reported by Shaw for the conversion of auricyanide to aurocyanide by glutathione.[10] Hence, multiple equilibria will be established in any system containing gold(I) thiolate complexes and disulfides, at least in principle (Scheme 3). However, gold(I) dithiolate complexes are also known to undergo loss of a ligand, probably via protonation of the lost ligand at sulfur, to form oligomeric gold(I) thiolate species, $[Au(SR)]_n$. This latter species is essentially insoluble and, hence, removed from the equilibrium system as it is formed. Therefore, a series of competitions are created, with the observed outcome decided by both the relative magnitude of the various equilibrium constants involved and Le Chatelier's principle.

For example, if K_1 is large and K_2 small, the oxidative addition product will dominate. In contrast, if K_1 is small and K_2 large, the outcome will be determined by the relative magnitudes of K_2 and K_1^{-1}: for $K_2 > K_1^{-1}$, a ligand exchange to produce a new gold(I) complex will be seen; for $K_1^{-1} > K_2$, the result would be no *apparent* reaction, at least over the relatively short time periods of the study, as the dominant solution species would be the starting gold(I) complex. A slightly more complex picture arises if mixed ligand systems are considered (i.e., the process designated by equilibrium constant K_3). Additionally, a new reaction pathway (A or B in Scheme 3) becomes operable if the metal-bound sulfur atom is a strong enough base to compete for a proton with other solution species, including the solvent. Such a pathway, if operable, leads to loss of a ligand and the formation of insoluble oligomeric $[RSAu]_n$. The resulting removal of gold species from the solution equilibrium system drives the overall process toward the oligomeric product, as required by Le Chatelier's principle. In the cases of the tetra- or pentafluorinated thiols, the very low basicity at sulfur ($pK_a \sim 4$) implies that protonation is not significant under the conditions employed and little to no oligomer should be observed. In contrast, if $[Au(AcMeCys)_2]^-$ forms at any point, it will be protonated to a much greater extent ($pK_a \sim 8$) and hence efficiently form an oligomer, as is indeed observed. In intermediate cases such as $[(PhS)_2Au]^-$, the outcome is likely to be highly sensitive to the reaction conditions, particularly with respect to the presence of a proton source.

Conclusion

The use of highly fluorinated electron-deficient ligands has allowed us to demonstrate, for the first time, the role that oxidative addition and reductive elimination processes play in the reactivity of gold thiolate complexes. Given the facile nature of the observed reactions, it is plausible that ligand substitution reactions at gold(I) in a variety of systems, including biological systems, undergo substitution processes by such an addition−elimination process via transient gold(III) intermediates rather than by a direct substitution process as has been previously hypothesized. Furthermore, these results demonstrate that fine control over reactivity at the gold center is possible via tuning of ligand electronics. Such information should prove useful in the further development of catalytically active gold complexes, an area of much current attention.[30]

Acknowledgment. The authors thank The University of the South and Georgetown University for financial support of this work. Funding for the purchase of the diffractometer was provided by the National Science Foundation and Georgetown University. R.E.B. thanks Amy Barrios as well as Alice and Mitchell Bruce for fruitful discussions.

Supporting Information Available: Complete tables of crystal data, positional parameters, bond distances and angles, and anisotropic displacement parameters for **1** and **2** as well as UV−vis data for **2** and **3**; X-ray crystallographic data, in CIF format, for **1a**,**b** and **2a**,**b**. This information is available free of charge via the Internet at http://pubs.acs.org. The X-ray crystallographic files have also been deposited with CCDC (ref. 668528−668531).

JA805266R

(30) (a) Della Pina, C.; Dimitratos, N.; Falletta, E.; Rossi, M.; Siani, A. *Gold Bull.* **2007**, *40*, 67–72. (b) Pichugina, D. A.; Kuzμmenko, N. E.; Shestakov, A. F. *Gold Bull.* **2007**, *40*, 115–120. (c) Richard, L. L.; Gagosz, F. *Organometallics* **2007**, *26*, 4704–4707. (d) Ray, L.; Shaikh, M. M.; Ghosh, P. *Organometallics* **2007**, *26*, 958–964. (e) Witham, C. A.; Mauleon, P.; Shapiro, N. D.; Sherry, B. D.; Toste, F. D *J. Am. Chem. Soc.* **2007**, *129*, 5838–5839.